JACS Au
AN OPEN ACCESS JOURNAL OF THE AMERICAN CHEMICAL SOCIETY

pubs.acs.org/jacsau
Article

Developing Aptamer-Based Colorimetric Opioid Tests

Juan Canoura, Obtin Alkhamis, Matthew Venzke, Phuong T. Ly, and Yi Xiao*

Cite This: JACS Au 2024, 4, 1059−1072
Read Online

ACCESS | Metrics & More | Article Recommendations | Supporting Information

ABSTRACT: Opioids collectively cause over 80,000 deaths in the United States annually. The ability to rapidly identify these compounds in seized drug samples on-site will be essential for curtailing trafficking and distribution. Chemical reagent-based tests are fast and simple but also notorious for giving false results due to poor specificity, whereas portable Raman spectrometers have excellent selectivity but often face interference challenges with impure drug samples. In this work, we develop on-site sensors for morphine and structurally related opioid compounds based on in vitro-selected oligonucleotide affinity reagents known as aptamers. We employ a parallel-and-serial selection strategy to isolate aptamers that recognize heroin, morphine, codeine, hydrocodone, and hydromorphone, along with a toggle-selection approach to isolate aptamers that bind oxycodone and oxymorphone. We then utilize a new high-throughput sequencing-based approach to examine aptamer growth patterns over the course of selection and a high-throughput exonuclease-based screening assay to identify optimal aptamer candidates. Finally, we use two high-performance aptamers with K_D of ∼1 μM to develop colorimetric dye-displacement assays that can specifically detect opioids like heroin and oxycodone at concentrations as low as 0.5 μM with a linear range of 0−16 μM. Importantly, our assays can detect opioids in complex chemical matrices, including pharmaceutical tablets and drug mixtures; in contrast, the conventional Marquis test completely fails in this context. These aptamer-based colorimetric assays enable the naked-eye identification of specific opioids within seconds and will play an important role in combatting opioid abuse.

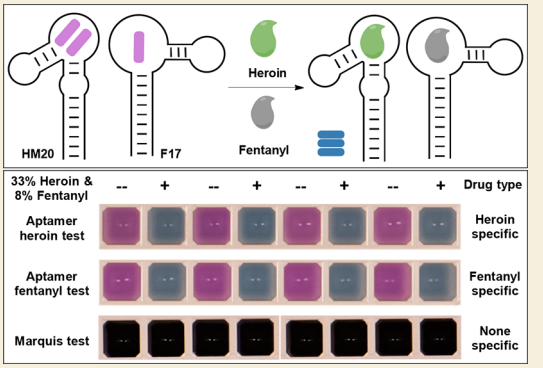

KEYWORDS: *aptamers, SELEX, opioids, high-throughput sequencing, exonuclease, dye-displacement assay, 3,3′-di(3-sulfopropyl)-4,5,4′,5′-dibenzo-9-methyl-thiacarbocyanine, Marquis test*

INTRODUCTION

Identifying and quantifying substances is crucial for a wide variety of applications such as medical diagnostics, quality control, and environmental monitoring.[1] In the field of forensics, advances in modern analytical techniques have allowed for unprecedented insights into the crime scene, such as through the detection of trace amounts of biological fluids, drugs, genetic material, and explosives.[2] Most progress, however, has been isolated to crime laboratories, while tantamount advances in analytical technologies that can be deployed on-site have severely lagged. For instance, the identification of drugs in seized substances in the field is still based on wet chemical techniques developed over a century ago.[3] Although these approaches are quick and easy to perform, they are notoriously prone to false results because the reagents employed in these tests react with generic functional groups that are shared by a broad range of compounds, such as aromatic rings, amines, phenols, and indoles.[4] One common chemical test is the Marquis test, which is often used to identify morphine-like opioids and entails mixing a drug sample with formaldehyde and sulfuric acid, where the resulting reaction results in two opioid molecules being joined together by formaldehyde to form a more extensively conjugated purple-colored cation product.[5] The test, however, is prone to false positives and negatives in response to cutting agents, adulterants, and other drugs of abuse. For instance, the test yields similar colors to those generated by opioids for diverse substances such as acetylsalicylic acid, 3,4-methylenedioxymethamphetamine (MDMA), and lysergic acid diethylamide (LSD).[4,6] When challenged with street drugs, which are typically low in purity, these tests also suffer from interference due to the mixing and/or masking of the color produced by the drug with that arising from other substances that generate their own distinct colors.[4,6,7] Lateral-flow immunoassays have recently emerged as a superior alternative for drug detection in solid substances, particularly for fentanyl. Although more specific than chemical tests, immunoassays have also been shown to cross-react to interferents like methamphetamine, MDMA, and diphenhydramine.[8] Recently,

Received: December 15, 2023
Revised: February 9, 2024
Accepted: February 14, 2024
Published: March 1, 2024

portable Raman spectrometers have been employed to identify drugs like opioids based on inelastic scattering of light resulting from vibrational transitions between ground and virtual excited states.[9] This approach is potentially very powerful because each molecule has its own unique Raman spectrum, which makes it highly specific. Raman spectrometers excel at identifying pure drugs; however, they face difficulties with highly impure, heavily adulterated drug samples,[10,11] and generally have poor detection limits, precluding the detection of drugs such as fentanyl, which may be present at only trace amounts.[12] Surface-enhanced Raman spectroscopy can overcome some of these issues but entails extra costs for specialized test kits and involves a more complex testing procedure.[12]

Approaches based on bioreceptors could enable the specific and sensitive detection of drug molecules because bioreceptors recognize their target by interacting with multiple functional groups of the target in space.[13] The most commonly employed bioreceptors, antibodies, are generated via in vivo immune processes, which enable little to no control over the binding profile of the resulting antibody.[14] As a result, they can sometimes cross-react with molecules other than the target. In addition, they are expensive and prone to batch-to-batch variation, have short shelf lives, and denature at higher temperatures or under harsh conditions.[15] Nucleic-acid-based bioreceptors known as aptamers have the potential to overcome current challenges associated with drug detection. They are oligonucleotide receptors that bind to specific molecules with high affinity and are isolated from randomized libraries through a method termed systematic evolution of ligands by exponential enrichment (SELEX).[16,17] Since SELEX is performed in vitro, the selection conditions and protocol can be manipulated in order to obtain aptamers that have high specificity toward one target[18] or even a family of compounds[19] while not responding to interferents that are commonly observed in many testing contexts. Aptamers also have other advantages including low cost of production, minimal batch-to-batch variation, and high stability.[15] There are several sensing platforms that are uniquely suited to aptamers, such as electrochemical aptamer-based sensors[20] and dye-displacement assays,[21] which can enable the rapid and simple detection of arbitrary analytes. For instance, we have used recently isolated aptamers that bind to fentanyl and several of its analogs to develop electrochemical and optical sensors that can detect nanomolar quantities of these drugs.[22,23]

In this work, we utilized SELEX to isolate aptamers that bind to morphine-like opioids and then used these aptamers to develop colorimetric sensors for these targets. We first used the parallel-and-serial selection[19] and toggle-selection[24] strategies to isolate two different sets of aptamers with differing binding profiles. High-throughput sequencing (HTS) of the selection pools revealed a variety of aptamer candidates, which we subsequently screened for their binding properties using an exonuclease digestion fluorescence assay.[25,26] We determined that one set of aptamers binds morphine, codeine, heroin, hydrocodone, and hydromorphone, while another set binds hydrocodone, hydromorphone, oxycodone, and oxymorphone. We then characterized the binding affinity of these aptamers using the gold-standard approach isothermal titration calorimetry (ITC) and utilized a set of high-quality aptamers to develop dye-displacement assays. We observed that our aptamer-based dye-displacement assay could detect heroin, fentanyl, and pharmaceutical opioids by the naked eye via a color change that occurs within seconds, with no response to structurally similar drug molecules dextromethorphan, cocaine, methamphetamine, acetaminophen, and methadone. To demonstrate the utility of our assay, we compared its sensing performance to that of the Marquis test. Our aptamer assay could identify minute quantities of fentanyl (8%) in heroin samples and oxycodone directly in excipient-rich pharmaceutical tablets. In contrast, the Marquis test completely failed these tests. Finally, we simplified assay procedures to an extent such that laypersons, such as law enforcement officials, can easily perform opioid testing outside of laboratory settings. Therefore, the aptamers and assays developed here will be of great use for the screening of morphine-like opioids in seized substances for forensic drug analysis.

MATERIALS AND METHODS

Reagents and Materials

Molecular biology grade water was purchased from Corning. Ultrapure water with a resistivity of 18.2 MΩ·cm was obtained from a Milli-Q EQ 7000 water purification system. Exonuclease I (Exo I, *E. coli*; 20 U/μL) and T5 exonuclease (T5 Exo; 10 U/μL) were purchased from New England Biolabs. Morphine sulfate hydrate, codeine phosphate hydrate, heroin HCl, oxycodone HCl, oxymorphone HCl, hydrocodone HCl, hydromorphone HCl, acetyl fentanyl HCl, fentanyl HCl, diazepam, alprazolam, clonazepam, (+)-methamphetamine HCl, ethylone HCl polymorph B, and methylnaltrexone bromide were purchased from Cayman Chemicals. Acetaminophen, benzocaine HCl, caffeine, cocaine HCl, chlorpromazine HCl, diphenhydramine HCl, lactose, mannitol, lidocaine HCl, naloxone HCl, naltrexone HCl, quinine hemisulfate monohydrate, and sodium dodecyl sulfate were purchased from Sigma-Aldrich. Noscapine HCl was purchased from the Tokyo Chemical Industry. Papaverine HCl was purchased from Acros Organics. Levamisole and xylazine HCl were purchased from MP Biomedicals. GoTaq Hot Start Master Mix was purchased from Promega. The QIAquick PCR purification kit was purchased from Qiagen. SYBR Gold, streptavidin-coated agarose resin (capacity: 1−3 mg biotinylated BSA/mL resin), 0.5 M EDTA solution (pH 8.0), sulfuric acid (trace metals grade), formaldehyde (37 wt %), and formamide were purchased from Thermo Fisher Scientific. 3,3′-di(3-sulfopropyl)-4,5,4′,5′-dibenzo-9-methyl-thiacarbocyanine (MTC) was synthesized in our laboratory. All other chemicals were purchased from Sigma-Aldrich unless otherwise specified.

Handling of Opioid Analytes

Fentanyl is a potent opioid that could prove dangerous if mishandled, and we followed precautions detailed in previous work to handle this compound.[23] Morphine-like opioids such as heroin, oxycodone, and hydrocodone are less potent, and we therefore used standard personal protective equipment (e.g., nitrile gloves, lab coat, long pants, and closed-toe shoes) when handling these substances.

Oligonucleotides

DNA oligonucleotides were purchased from Integrated DNA Technologies with standard desalting purification. The random library, PCR primers, and biotinylated 18-nt complementary DNA (cDNA15-bio) were HPLC purified. The random library was ordered as machine-mixed. High-throughput sequencing data showed that the nucleotides of the random region consisted of 22, 28, 22, and 28% of A, T, C, and G, respectively (Figure S1). DNA was dissolved in molecular biology grade water, and their concentrations were determined using a NanoDrop 2000 Spectrophotometer (Thermo Fisher Scientific). These oligonucleotide sequences can be found in Table S1.

Buffers

All experiments were performed in selection buffer [10 mM Tris−HCl (pH 7.4), 20 mM NaCl, and 0.5 mM $MgCl_2$]. For dye

https://doi.org/10.1021/jacsau.3c00801
JACS Au 2024, 4, 1059−1072

displacement experiments, the selection buffer included 1% (v/v) DMSO and 0.01% (w/v) SDS as a surfactant. Quenching solution for exonuclease digestion assays contained 10 mM Tris−HCl (pH 7.4), 21 mM EDTA, 12.5% (v/v) formamide, and 1× SYBR Gold (final concentrations).

Library-Immobilized Selection for Isolating Morphinan-Based Opioid-Binding Aptamers

A library-immobilized selection strategy was employed as previously described.[27] For each round, the library was mixed with a 5-fold excess of cDNA15-bio in selection buffer, heated to 90 °C for 10 min, and slowly cooled to room temperature over 20 min in a water bath to promote annealing. The library-cDNA complex was then immobilized onto streptavidin-coated agarose beads loaded in a gravity column (0.8 mL) and preconditioned with selection buffer. The library-bead assembly was washed several times with the selection buffer to remove nonspecifically eluting library strands. Counter-SELEX was performed from round 2 onward to remove aptamers that bind to interferents. Afterward, positive selection with the target was performed by adding the target to the column and collecting all eluted library molecules. These eluted strands were PCR-amplified under the following reaction conditions: 2 min at 95 °C; 11 cycles of 95 °C for 15 s, 58 °C for 30 s, and 72 °C for 45 s; and finally, 5 min at 72 °C. Successful PCR amplification of the library was confirmed using agarose gel electrophoresis. The amplicons were then converted to single-stranded DNA using streptavidin-coated agarose resin and NaOH treatment.[27] Finally, the pool was subjected to another round of SELEX. Pool affinity and specificity were periodically assessed using a previously reported gel-elution assay.[28] Binding curves were fitted with a modified one-site Langmuir equation:

$$y = S + (E - S)\frac{x^n}{x^n + k^n}$$

where y is the percentage of pool elution, S represents pool elution at a ligand concentration of zero, E represents the maximal value of pool elution, x is the ligand concentration, k is the ligand concentration producing half-maximal pool elution, and n is the Hill coefficient.

Parallel-and-serial selection was employed to isolate cross-reactive aptamers for heroin and morphine. First, parallel selection was performed using heroin or morphine for six rounds to pre-enrich individual pools, after which a gel elution assay[28] was performed to confirm target binding. To perform serial selection, 150 pmol of each of the round 6 heroin and morphine pools were mixed and challenged with heroin for one round, followed by morphine in the next round. This selection was then repeated for rounds 3 and 4 of the serial selection. A gel elution assay was used to determine the binding affinity and specificity of the final pool. Details about the selection conditions can be found in Tables S2−S4.

For the isolation of cross-reactive aptamers for oxycodone and oxymorphone, a pool was first enriched using only oxycodone as the target for six rounds. Then, a toggle selection strategy was applied, such that in the seventh round, oxymorphone was used as the selection target, followed by oxycodone during the eighth round. The selection target was subsequently toggled between oxycodone or oxymorphone for four additional rounds, after which the pool affinity and specificity were confirmed using a gel elution assay. Details about selection conditions can be found in Tables S5 and S6.

High-Throughput Sequencing

Serial selection rounds S0−4 for the morphine and heroin pools and toggle selection rounds T0, T1, T2, T3, T4, and T6 for the oxycodone and oxymorphone pools were subjected to Illumina-based HTS by Azenta Life Sciences. Prior to submission, partial Illumina adapters were added to each sequence via PCR amplification using customized forward and reverse primers (Table S1, FP-HTS and RP-HTS). Specifically, 100 nM of each pool was mixed with 1 μM FP-HTS and RP-HTS and subjected to 10 PCR cycles under the following conditions: 2 min at 95 °C; 9 cycles at 95 °C for 15 s, 58 °C for 30 s, and 72 °C for 45 s; and finally, 5 min at 72 °C. The PCR product was confirmed using polyacrylamide gel electrophoresis (PAGE) and then purified using the QIAquick PCR purification kit. A 20 ng/μL solution of the purified pool was submitted for sequencing. For analysis, the constant regions were removed from each pool using cutadapt software.[29] FASTAptamer[30] was then used to obtain the population of each unique sequence during SELEX as well as its enrichment-fold between rounds.

Exonuclease Digestion Fluorescence Assay for Aptamer Affinity Screening

The exonuclease digestion fluorescence assay was performed as previously described.[31] The aptamer (final concentration: 0.5 μM) was first diluted in Tris buffer (final concentration: 10 mM, pH 7.4), heated to 95 °C for 10 min, and immediately cooled on ice for 1 min. NaCl (final concentration: 20 mM), $MgCl_2$ (final concentration: 0.5 mM), and BSA (final concentration: 0.1 mg/mL) were then immediately added. 5 μL of the aptamer solution was then added to 20 μL of buffer, target, or interferent dissolved in selection buffer at various concentrations. The mixture was incubated at 25 °C for 30 min, after which 25 μL of selection buffer containing T5 and Exo I (final concentrations: 0.2 and 0.015 U/μL, respectively) plus 0.1 mg/mL BSA was added to begin the digestion reaction. 5 μL of the sample was collected at various time points and added to 30 μL of quenching solution in the wells of a 384-well black microplate. SYBR Gold fluorescence was recorded using a Tecan Spark plate reader with an excitation wavelength of 495 nm and an emission wavelength of 537 nm. The fluorescence was plotted against each time point to construct the time-course digestion plots of each sample. Enzymatic inhibition was measured in terms of resistance value, which is calculated using the formula $(AUC_t/AUC_0) - 1$, where AUC_t and AUC_0 are the areas under the curve of the time-course data with and without the target, respectively. The integration time was customized for each aptamer and chosen as the point at which fluorescence reached 10% of its initial value for the blank sample. The fluorescence of each sample was recorded 10 times, and average values were used for analysis.

Determination of Aptamer Binding Affinities Using Isothermal Titration Calorimetry

ITC experiments were performed in selection buffer at 23 °C using a Malvern MicroCal iTC200 instrument. Aptamer and target concentrations used for ITC experiments are described in Table S7 for heroin-binding (HM) aptamers and Table S8 for oxycodone-binding (OM) aptamers. 320 μL of aptamer in 10 mM Tris buffer (pH 7.4) was heated to 95 °C for 10 min and then cooled immediately on ice for 1 min. 40 μL of 10× NaCl and 40 μL of 10× $MgCl_2$ were then added to reach the final selection buffer conditions. 300 μL of the solution was loaded into the cell, and the syringe was loaded with a minimum of 38.4 μL of either morphine or oxycodone dissolved in selection buffer. During ITC experiments, an initial purge injection of 0.4 μL was performed followed by 19 successive injections of 2 μL with a spacing of 180 s between each injection. The data were then fitted with a one-site binding model using the MicroCal analysis kit integrated into Origin 7 software.

Optimization of Aptamer Concentration for the MTC Displacement Assay

Each dye displacement sensor was first tested to identify the optimal aptamer-to-dye ratio as previously described.[32] First, a 99 μL solution of HM20 or OM9 was prepared at various concentrations (0, 1, 2, 3, 4, 5, 6, 7, 8, 9, and 10 μM) in 1.01× selection buffer containing SDS (final concentration: 0.01% w/v) and incubated at room temperature for 5 min. 1 μL of 250 μM MTC dissolved in DMSO was added directly to the solution and rapidly mixed. 72 μL of this mixture was then loaded into the wells of a transparent 384-well microplate, and the absorbance spectra were recorded using a Tecan Spark microplate reader from 400−800 nm with a 5 nm step size.

Detection of Opioids Using a Colorimetric MTC Displacement Aptamer Assay

The optimal aptamer concentrations for our dye displacement sensors were 6 and 4 μM for HM20 and OM9, respectively. Each aptamer was

https://doi.org/10.1021/jacsau.3c00801
JACS Au 2024, 4, 1059−1072

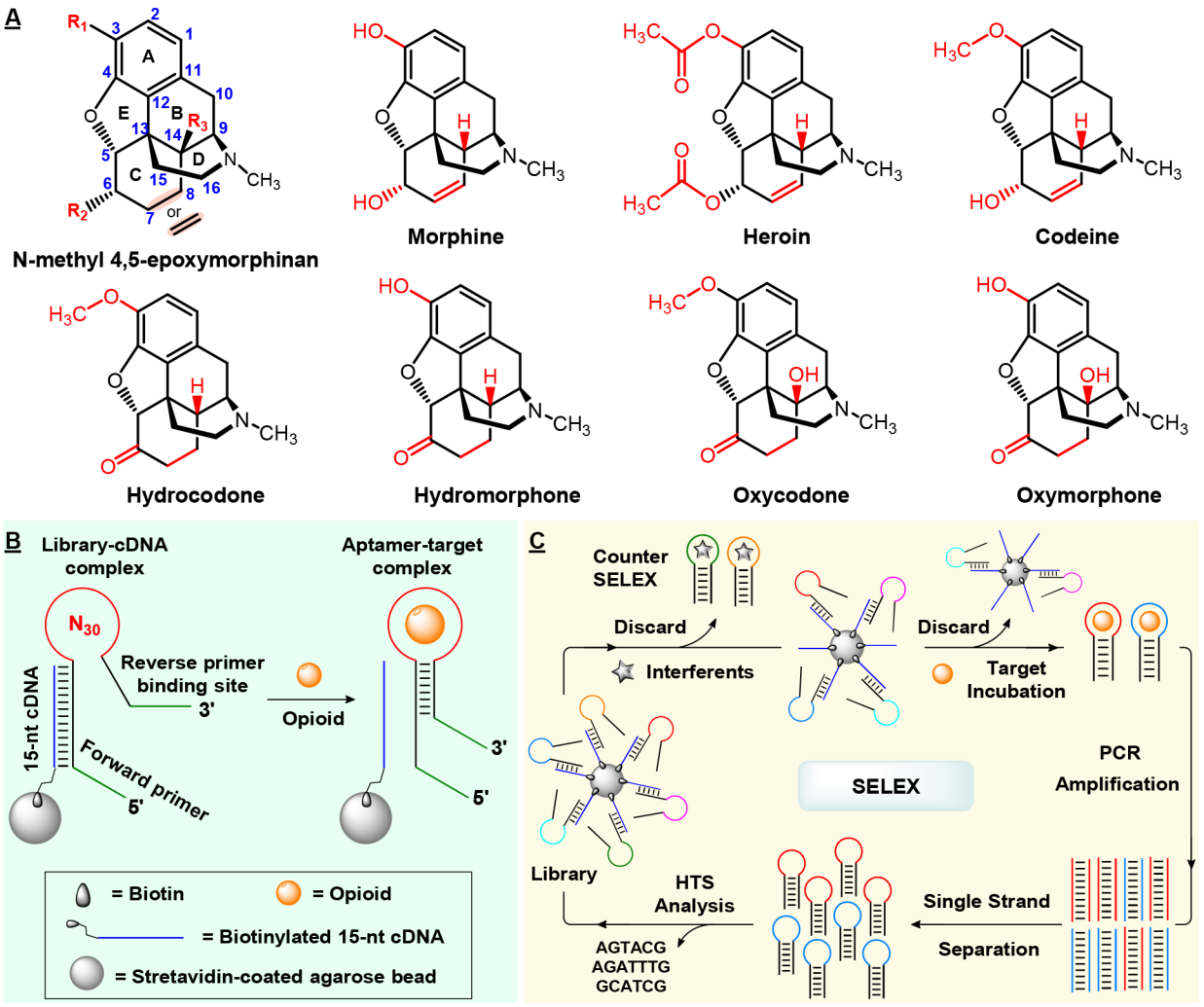

Figure 1. SELEX targets and selection strategy. (A) Structure of the opioid targets. All opioids share the 4,5-epoxymorphinan core structure (drawn in black) and vary at the indicated R groups and bond orders between C7 and C8 (indicated in red). Atom positions are numbered in blue. (B) Library design. (C) Working principle of library-immobilized SELEX.

diluted to a volume of 39.2 μL at their respective concentrations in 1.01× selection buffer containing SDS (final concentration: 0.01% (w/v)) and incubated at room temperature for 5 min, after which 0.8 μL of 250 μM MTC in DMSO was added and rapidly mixed. The mixture was then added to 40 μL of SDS-containing buffer with or without a target (heroin for HM20, oxycodone for OM9). Final target concentrations were 0, 0.5, 1, 2, 4, 8, 16, 32, 64, 128, 256, and 512 μM. Finally, 72 μL of the sample was loaded into the wells of a transparent 384-well microplate, and the absorbance spectra were recorded, as described above.

For specificity testing, the aptamer-dye complexes were prepared using the same protocol, after which the mixture was added to 40 μL of buffer containing 0.01% SDS, 25 μM target (oxycodone for OM9 and heroin for HM20) in buffer containing 0.01% SDS, or 50 μM interferent (lactose, mannitol, cocaine, benzocaine, naloxone, methylnaltrexone, levamisole, lidocaine, fentanyl, procaine, (+)-pseudoephedrine, diphenhydramine, (+)-methamphetamine, acetaminophen, xylazine, ethylone, alprazolam, diazepam, clonazepam, papaverine, noscapine, quinine, or caffeine) in buffer containing 0.01% SDS. For binary mixture testing, the aptamer-dye complexes were prepared using the same protocol, after which the mixture was added to 40 μL of buffer containing 0.01% SDS, 25 μM target (oxycodone for OM9 and heroin for HM20) dissolved in buffer containing 0.01% SDS, or 25 μM target mixed with 50 μM interferent (lactose, mannitol, cocaine, benzocaine, naloxone, naltrexone, methylnaltrexone, levamisole, lidocaine, fentanyl, procaine, (+)-pseudoephedrine, diphenhydramine, (+)-methamphetamine, acetaminophen, xylazine, ethylone, alprazolam, diazepam, clonazepam, papaverine, noscapine, quinine, or caffeine) in buffer containing 0.01% SDS.

Extraction of Pharmaceutical Pill Contents

Pills tested include Advil (200 mg of ibuprofen), Claritin (10 mg of loratadine), Benadryl (25 mg of diphenhydramine), Mucinex (60 mg of dextromethorphan and 1200 mg of guaifenesin), Tylenol (325 mg of acetaminophen), generic hydrocodone (Tris Pharma Inc., G035; 5 mg of hydrocodone and 325 mg of acetaminophen), and generic oxycodone (4839 V; 5 mg of oxycodone and 325 mg of acetaminophen). Each pill was placed in its own Ziploc bag and gently crushed into a fine powder. The bag contents were then transferred into a 25 mL centrifugation tube after dissolving in 10 mL of DI water containing 10% MeOH (v/v) and allowed to extract for 30 min at room temperature on an end-over-end rotator. The extract was then centrifuged at 5000 rcf for 10 min, and the supernatant was filtered using a 0.45-μm MCE syringe filter.

Detection of Opioids in Pill Extracts Using an Aptamer-Based MTC Displacement Assay

OM9 was utilized for oxycodone detection using the optimal aptamer concentration. The aptamer was diluted to a volume of 39.2 μL in 1.01× selection buffer containing SDS (final concentration: 0.01% (w/v)) and allowed to sit at room temperature for 5 min, after which 0.8 μL of 250 μM MTC in DMSO was added and rapidly mixed. The mixture was then added to 40 μL of pill extract diluted 5-fold in

https://doi.org/10.1021/jacsau.3c00801
JACS Au 2024, 4, 1059−1072

selection buffer. Finally, 72 μL of the sample was loaded into the wells of a transparent 384-well microplate, and the absorbance spectra were recorded as described above.

Detection of Mock Heroin Mixtures Using the Marquis Reagent

The Marquis reagent was prepared freshly before use.[6] Briefly, 1 mL of concentrated sulfuric acid was added to 50 μL of formaldehyde (37%) to create the working solution. Then, 100 μL of the working solution was added to 0.5 mg of solid powder pure drug (heroin or fentanyl), interferent (caffeine, lidocaine, mannitol, or lactose), binary mixtures containing 33% heroin and 67% of one of the four interferents, binary mixtures containing 8% fentanyl and 92% of one of four interferents, or ternary mixtures containing 33% heroin, 8% fentanyl, and 59% of one of four interferents (all percentages are based on mole percent). The reaction was allowed to proceed for at least 1 min, after which photographs were obtained with a Nikon D750 camera.

Detection of Pharmaceutical Pills Using the Marquis Reagent

The Marquis reagent was prepared freshly before use, as explained above. The tested pills included Advil (200 mg of ibuprofen), Claritin (10 mg of loratadine), Benadryl (25 mg of diphenhydramine), Mucinex (60 mg of dextromethorphan and 1200 mg of guaifenesin), Tylenol (325 mg of acetaminophen), generic hydrocodone (Tris Pharma Inc., G035) (5 mg of hydrocodone and 325 mg of acetaminophen), and generic oxycodone (4839 V) (5 mg of oxycodone and 325 mg of acetaminophen). Samples were collected by breaking each tablet into fourths and scraping off ∼1 mg of tablet material with a spatula. Then, 100 μL of the working solution was added to the obtained solid powder and allowed to react for 1 min before taking photographs.

On-Site Detection of Pharmaceutical Pills Using a Colorimetric Dye Displacement Aptamer Assay

For a field test for determining opioids in tablets, OM9 (final concentration = 4 μM) was diluted to a volume of 89 μL in 1.1× selection buffer containing SDS (final concentration: 0.01% (w/v)), after which 1 μL of 250 μM MTC in DMSO was added and rapidly mixed. The tablets mentioned above were broken into fourths, and ∼1 mg of pill material was obtained by scraping its contents using a spatula and adding it to a 0.2 mL tube. Subsequently, 20 μL of 10% MeOH (v/v) in deionized water was added to the tube, and the contents were vigorously shaken for 1 min, after which 10 μL of the slurry was added to 90 μL of the aptamer dye solution. Samples were then loaded into a 384-well white plate, and photographs were obtained.

RESULTS AND DISCUSSION

Choice of Selection Targets

Opioids with structural similarity to morphine include the opiate codeine and the semisynthetic opioids heroin, hydrocodone, hydromorphone, oxycodone, and oxymorphone. Morphine, codeine, heroin, hydrocodone, and hydromorphone share the same *N*-methyl 4,5-epoxymorphinan core structure, while oxycodone and oxymorphone contain a similar, yet distinct, core that contains a hydroxyl group at carbon 14 (C14) in place of hydrogen (Figure 1A). We categorized these seven targets into two groups based on the differences in their core structure. Our goal was to isolate two different aptamers that could recognize these two different core structures while tolerating alterations at other substituent sites. Ideally, these two aptamers combined should be cross-reactive to all seven opioids with minimal false responses. Therefore, we performed two independent selections using representative molecules from each subfamily: one using morphine and heroin as targets and the other using oxycodone and oxymorphone as targets.

Isolation of Cross-Reactive Aptamers via Parallel-and-Serial Selection Using Morphine and Heroin

We performed library-immobilized SELEX with a 73-nucleotide (nt) stem-loop-structured DNA library as previously reported.[27] Each library molecule contains a 30-nt random domain serving as the putative binding domain, flanked by an 8-base-pair (bp) stem with two PCR primer-binding sites at both termini. The library can hybridize to an 18-nt biotinylated complementary DNA, which we termed cDNA15-bio because it forms a 15-bp duplex with the library sequences, facilitating immobilization of the library-cDNA complex onto streptavidin-coated agarose beads. Upon binding of the selection target to a library strand, the aptamer undergoes a conformational change, is displaced from the cDNA, and is released into solution (Figure 1B). These target binders are then collected and PCR-amplified to generate a new single-stranded pool for another round of selection until the pool displays high affinity for the target(s) (Figure 1C).

To enrich aptamers that can broadly recognize morphine-related opioids, we utilized the parallel-and-serial selection strategy that we employed previously to isolate class-specific aptamers for the synthetic cathinone drug family.[19] This strategy includes two steps: the first step is to generate two different pools, where each is enriched against an individual target (i.e., parallel selection). The second step is to combine these two pre-enriched pools and challenge the merged pool with two targets sequentially (i.e., serial selection). Specifically, we first performed two independent selections using morphine and heroin as targets in parallel for six rounds to enrich target-binding sequences (Figure S2A, rounds P1−P6). For rounds P1−P5, we employed 500 μM target, reducing the target concentration to 250 μM in round P6. Beginning from round P2, counter-SELEX was performed to remove binders to interferents commonly found in seized substances such as cutting agents (caffeine, lactose, and mannitol), adulterants (quinine, chlorpromazine, procaine, lidocaine, benzocaine, diphenhydramine, levamisole, acetaminophen, and xylazine), controlled substances (cocaine, diazepam, alprazolam, clonazepam, acetyl fentanyl, (+)-methamphetamine, (+)-pseudoephedrine, and ethylone), endogenous compounds in the opium plant (papaverine and noscapine), and opioid receptor antagonists (naloxone, naltrexone, and methylnaltrexone) (see Figure S3 for chemical structures). Counter-targets were used at a concentration of 200−500 μM and were employed individually or as a group; detailed selection conditions are provided in Tables S2 and S3. During rounds P1−P6, the proportion of pool eluted by the targets was relatively low, even when adjusted per micromolar target concentration (0.3−2%; Figure S2B). However, certain counter-targets such as papaverine and noscapine eluted a sizable quantity of pool during these rounds, ranging from 8−23%. This can be attributed to the fact that these substances are capable of nonspecifically binding double-stranded DNA.[33,34] We employed a gel elution assay to determine the target-binding affinity of round P5 and P6 heroin and morphine pools. For both P5 pools, we observed no binding to their respective targets, indicating that these pools had not been sufficiently enriched with target binders to be detectable by our gel-elution assay (Figure S4A,B). However, the Round P6 heroin and morphine pools displayed dissociation constants (K_D) of 50 μM (Figure S4C) and 30 μM (Figure S4D), respectively, with maximum elution of ∼14% for their respective targets.

https://doi.org/10.1021/jacsau.3c00801
JACS Au 2024, 4, 1059−1072

We then combined an equimolar quantity of the heroin and morphine round P6 pools (Figure S2A, S0 pool) and performed two cycles of serial selection (Figure S2A, rounds S1−S4). Each cycle consisted of first challenging the pool with heroin and PCR-amplifying binders and then challenging the resultant pool with morphine. The rationale underlying this strategy is that aptamers that can recognize both targets—and perhaps target analogs like codeine, hydrocodone, and hydromorphone—will be preferentially enriched relative to those that bind only one target. In rounds S1 and S2, 50 μM heroin and morphine were used, while 25 μM was used for each target in rounds S3 and S4 (Table S4). For rounds S1 and S2, heroin eluted 4.5% of the pool, while morphine eluted 12.1%. In rounds S3 and S4, the size of the eluted fraction rose to 11.7% for heroin and 16.1% for morphine. The proportion of pool eluted per micromolar concentration of the target applied is shown in Figure S2B. We then characterized the binding affinity and specificity of the resulting S4 pool by using the gel-elution assay. The pool demonstrated a K_D of 14 and 6 μM for heroin and morphine (Figure S5), respectively, and had minimal response to most counter-targets at a 10-fold higher concentration relative to the targets, including naloxone, naltrexone, and methylnaltrexone; papaverine, noscapine, diazepam, alprazolam, and clonazepam were used at 4-fold higher concentration (Figure S2C). However, papaverine, noscapine, and diazepam demonstrated cross-reactivities of 14.8, 9.2, and 10.6%, respectively. Nevertheless, since the pool bound to the two selection targets with decent affinity, we concluded this selection.

Toggle Selection for Oxycodone and Oxymorphone Aptamers

We then performed a separate SELEX to isolate cross-reactive aptamers for oxycodone and oxymorphone. First, we pre-enriched a pool using oxycodone (Figure S2D, rounds R1−R6). We used 500 μM oxycodone for rounds R1 and R5, reducing this to 250 μM for R6. Oxycodone eluted a relatively low proportion of library during these rounds (0.4−1.2%; percentage of pool eluted per micromolar of the target is shown in Figure S2E). Starting from round R2, we performed counter-SELEX similar to the morphine-heroin selection (Table S5). Papaverine, noscapine, diazepam, and a combination of cocaine, lidocaine, and benzocaine eluted ∼20% of the pool in rounds R2−4. In rounds R4 and R6, chlorpromazine, acetyl fentanyl, and naloxone also demonstrated increased pool elution relative to earlier rounds. We determined the binding affinity of the round R5 and R6 pools using a gel-elution assay. Although the R5 pool did not have any affinity for oxycodone (Figure S6A), the R6 pool had a K_D of 81 μM and maximum pool elution of 12% (Figure S6B).

To enrich aptamers that cross-react to oxycodone and oxymorphone from the R6 pool (Figure S2D, T0 pool), we applied a previously reported toggle SELEX strategy which uses different targets during alternating rounds of selection.[24] Specifically, we first applied oxymorphone as a target followed by oxycodone in the next round, alternating targets every round for a total of six rounds (Figure S2D, rounds T1−T6). Detailed selection conditions are shown in Table S6. For rounds T1 and T2, 100 μM target was used, achieving 6 and 10% pool elution, respectively. However, when target concentration was reduced to 25 μM in rounds T3 and T4, pool elution, respectively, decreased to 3.8 and 5.6%. Nevertheless, the pools from these rounds exhibited greater elution when adjusted per micromolar concentration of the target relative to rounds T1−2 (Figure S2E). When target concentrations were further reduced to 10 μM in rounds T5 and T6, absolute pool elution rose again to 11.3 and 11.8%, respectively, indicating that cross-reactive aptamers were successfully being enriched. Throughout the toggle rounds, we noticed that papaverine, noscapine, and diazepam consistently eluted a considerable amount of the library. More importantly, the structurally similar counter-targets naloxone and naltrexone were responsible for the highest levels of pool elution, with an average of 5% for naloxone. After round T6, we performed the gel-elution assay to characterize the pool's binding properties and determined K_Ds of 8.7 and 10.1 μM for oxycodone and oxymorphone, respectively (Figure S7). This pool also demonstrated high specificity, with no response observed against 10-fold higher concentrations of most interferents, even naloxone (Figure S2F). Therefore, the toggle selection was successful in isolating cross-reactive aptamers for oxycodone and oxymorphone.

HTS Analysis and Affinity Measurement with ITC

Previous studies have shown that early pools from SELEX comprise a high percentage of unique sequences, making identification of aptamers challenging among the noise of nonbinding sequences.[35] We therefore submitted four serial selection pools from the heroin-morphine (HM) SELEX and five toggle selection pools from the oxycodone-oxymorphone (OM) SELEX for HTS. From the HM pools, we sequenced pools S0−4, obtaining 403,306,198,943, 189,690, 231,111, and 257,228 reads, respectively. For the OM pools, we sequenced T0−4 and T6, obtaining 493,257, 189,685, 219,578, 184,110, 185,984, and 159,168 reads, respectively. The diversity of sequences in the pool decreased considerably during selection, with the percentage of unique sequences in the serial selection HM pools decreasing from 28.4% in S0 to 1.1% in the final round and from 32.3% in T0 to 4.0% in T6 for the toggle-selection OM pools (Figure S8). Overall, the OM pool was less enriched in every round relative to the HM pool. Aptamer candidates were chosen from each pool based on their enrichment behavior. Specifically, candidates were separated into four categories based on evolutionary trends, in which sequence abundance: (1) continuously increased with an exponential or linear growth rate (Figure 2A,B), (2) consistently increased with a gradually diminishing growth rate (Figure 2C,D), (3) peaked at some point (Figure 2E,F), or (4) always decreased between rounds (Figure 2G,H). We hypothesized that aptamers from category 1 most likely had the highest target-binding affinities, whereas those from categories 2 and 3 would possess moderate binding affinity. For the final HM S4 pool, 41% of the pool was classified as category 1, 3.4% was in category 2, 30% was in category 3, 0.8% was in category 4, and 25% did not meet the criteria for any category (Figure S9). For the final OM T6 pool, 47% of the pool was classified as category 1, 15.5% was in category 2, 15.5% was in category 3, 3.5% was in category 4, and ∼18% did not meet the criteria for any category (Figure S10).

We selected the top 10 candidates from category 1 (five linear and five exponential), the top 10 candidates from category 2, and the top five candidates from category 3 from both the HM and OM pools for further affinity characterization. No sequences were selected from category 4, as these may have had weak affinity to the selection target or strong binding to a counter-target. For further characterization, we

https://doi.org/10.1021/jacsau.3c00801
JACS Au 2024, 4, 1059−1072

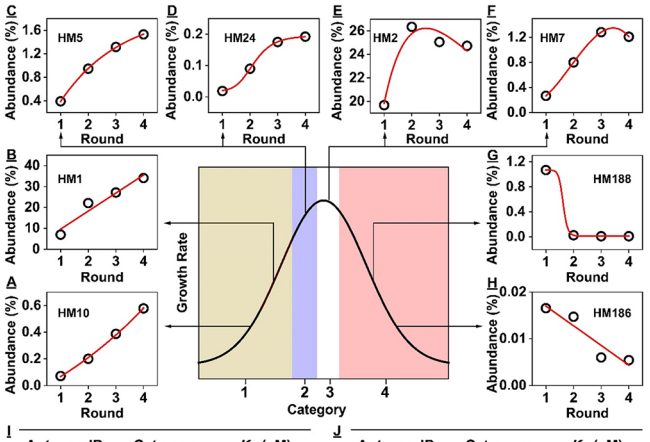

I

Aptamer ID	Category	K_D (μM)
HM10	1 (Exponential)	3.76 ± 0.4
HM20	1 (Exponential)	1.11 ± 0.06
HM116	1 (Exponential)	2.11 ± 0.11
HM383	1 (Exponential)	NA
HM426	1 (Exponential)	4.52 ± 0.21
HM1	1 (Linear)	0.85 ± 0.03
HM4	1 (Linear)	2.39 ± 0.25
HM9	1 (Linear)	2.4 ± 0.14
HM15	1 (Linear)	3.41 ± 0.15
HM16	1 (Linear)	1.61 ± 0.1
HM5	2	2.61 ± 0.22
HM11	2	4.35 ± 0.25
HM14	2	4.13 ± 0.5
HM23	2	3.11 ± 0.17
HM24	2	2.18 ± 0.1
HM29	2	2.67 ± 0.17
HM30	2	2.28 ± 0.2
HM31	2	5.62 ± 0.44
HM41	2	3.31 ± 0.28
HM54	2	NA
HM2	3	4.57 ± 0.25
HM7	3	4.74 ± 0.43
HM22	3	4.08 ± 0.33
HM25	3	6.49 ± 0.49
HM31.2	3	3.31 ± 0.28

J

Aptamer ID	Category	K_D (μM)
OM1	1 (Exponential)	0.45 ± 0.03
OM4	1 (Exponential)	0.99 ± 0.13
OM5	1 (Exponential)	0.41 ± 0.05
OM6	1 (Exponential)	0.5 ± 0.04
OM7	1 (Exponential)	1.42 ± 0.08
OM3	1 (Linear)	3.06 ± 0.29
OM8	1 (Linear)	2.22 ± 0.15
OM12	1 (Linear)	2.9 ± 0.15
OM15	1 (Linear)	1.69 ± 0.07
OM29	1 (Linear)	0.51 ± 0.03
OM2	2	0.9 ± 0.07
OM9	2	1.15 ± 0.06
OM10	2	1.06 ± 0.07
OM13	2	3.7 ± 0.28
OM14	2	2.16 ± 0.07
OM16	2	1.19 ± 0.13
OM22	2	1.75 ± 0.12
OM28	2	6.13 ± 0.43
OM31	2	3.19 ± 0.24
OM36	2	2.77 ± 0.13
OM11	3	0.79 ± 0.09
OM17	3	3.65 ± 0.21
OM19	3	2.43 ± 0.18
OM20	3	2.16 ± 0.19
OM25	3	6.29 ± 0.42

Figure 2. HTS analysis of enriched aptamer pools and binding affinity characterization of isolated aptamers. Four categories of aptamers were defined based on their growth pattern during SELEX: (A, B) exponential or linear growth (Category 1), (C, D) gradually reducing growth rate (Category 2), (E, F) peaked (Category 3), and (G, H) declining between rounds (Category 4). ITC-derived binding affinity of the 25 aptamers from categories 1, 2, and 3 isolated from (I) HM (for morphine) and (J) OM (for oxycodone) SELEX.

synthesized these aptamers as 46-nt constructs with 8-bp constant double-stranded stems and 30-nt loops, without PCR primer-binding sites (Tables S9 and S10). Based on our experience, this modification does not meaningfully affect aptamer affinity. We used the gold-standard method ITC[36] to determine the K_D of these 50 candidates against morphine for the HM aptamers (Figures S11−15) or oxycodone for the OM aptamers (Figures S16−S20). K_D values ranged from 0.84 to 6.49 μM and 0.41 to 6.30 μM for HM and OM aptamers, respectively (Figure 2I,J and Tables S7 and S8). On average, aptamers from category 1 had higher affinity than those in category 2 and 3. For example, the K_D values of HM aptamers from category 1 ranged from 0.84 to 4.52 μM, while those from category 2 ranged from 2.18 to 5.61 μM and category 3 ranged from 3.31 to 6.49 μM. A similar pattern held for the OM aptamers. Unexpectedly, while HM383 and HM54 were promising category 1 and 2 sequences, respectively, ITC indicated that they did not bind the target. Since these aptamers had very low read counts (473 and 38.8 reads per million, respectively), the use of enrichment-fold as a metric to assess aptamer quality might have been unreliable. These HTS data indicate that selecting aptamer candidates based on their growth rate throughout multiple later SELEX rounds, where the abundance of such sequences is sufficiently high that HTS could reliably quantify them,[35] might be a promising positive predictor of aptamer quality.

Binding Characterization of Aptamer Candidates Using an Exonuclease-Based Fluorescence Assay

We then characterized the binding properties of each aptamer candidate using a fluorescence assay based on the 5′-3′ DNA exonuclease, T5 Exonuclease (T5 Exo), and the 3′-5′ single-stranded DNA exonuclease, Exonuclease I (Exo I).[31] T5 Exo and Exo I digest DNA aptamers into mononucleotides in the absence of ligand, but digestion is inhibited when the aptamer is bound to a ligand in a manner dependent on ligand concentration and aptamer-ligand affinity (Figure 3A). Monitoring the digestion process over time (for instance, with a DNA-binding fluorescent stain like SYBR Gold) can provide a measure of ligand binding affinity and specificity.[22] We quantify this interaction using the metric resistance value (R_{value}), which is equal to the ratio of the area under the curve (AUC) of the digestion time-course plot with versus without target minus 1. We began by digesting each candidate with T5 Exo and Exo I in the absence or presence of 100 μM heroin for HM aptamers and 100 μM oxycodone for OM aptamers. In total, 22 HM candidates (Figure 3B) and 14 OM candidates demonstrated moderate to high enzymatic inhibition (R_{value} > 0.2) (Figure 3C). All other aptamers had little to no inhibition (R_{value} < 0.2). We next assessed the cross-reactivity of the 22 HM aptamers and 14 OM aptamers to seven opioid analogs (heroin, morphine, codeine, oxycodone, hydrocodone, oxymorphone, and hydromorphone) at a concentration of 100 μM using the T5/Exo I assay. Except for HM25, most HM aptamers demonstrated the ability to bind heroin, morphine, codeine, hydrocodone, and hydromorphone with similar levels of enzymatic inhibition. Only five aptamers (HM1 HM9, HM16, HM20, and HM24) also responded to oxycodone and oxymorphone with cross-reactivity of 40−60% (Figure 3D). All OM aptamers were able to bind oxycodone and oxymorphone with high cross-reactivity (80−112%), but these also had differing cross-reactivity for the other opioids. In particular, OM3, OM4, and OM5 also cross-reacted to hydrocodone and hydromorphone at a level of 80−130%, but these aptamers had a significantly weaker response to morphine, heroin, and codeine (<25% cross-reactivity) (Figure 3E).

We then assessed the specificity of these aptamers against the counter-targets at a concentration of 250 μM (100 μM for papaverine, noscapine, alprazolam, diazepam, clonazepam) relative to 100 μM target using the T5 Exo/Exo I assay. Most HM aptamers did not respond to the synthetic opioids fentanyl and acetyl fentanyl (Figure 3D), which is imperative for the practical use of these aptamers given that seized drugs and counterfeit medications are often adulterated with such substances.[37,38] HM2, HM4, HM20, HM29, HM30, and HM31 were the most specific aptamers, with cross-reactivities <10% to all tested interferents. The remaining HM aptamers had moderate to severe cross-reactivity to various counter-targets. Notably, although papaverine consistently eluted a large quantity of the pool during counter-SELEX, all aptamers had minimal cross-reactivity to this compound except for HM1 and HM31.2 (20−22% cross-reactivity). For the OM aptamers, OM3, OM4, OM9, OM14, OM16, and OM19 had high specificity against all interferents, even naloxone, with

https://doi.org/10.1021/jacsau.3c00801
JACS Au 2024, 4, 1059−1072

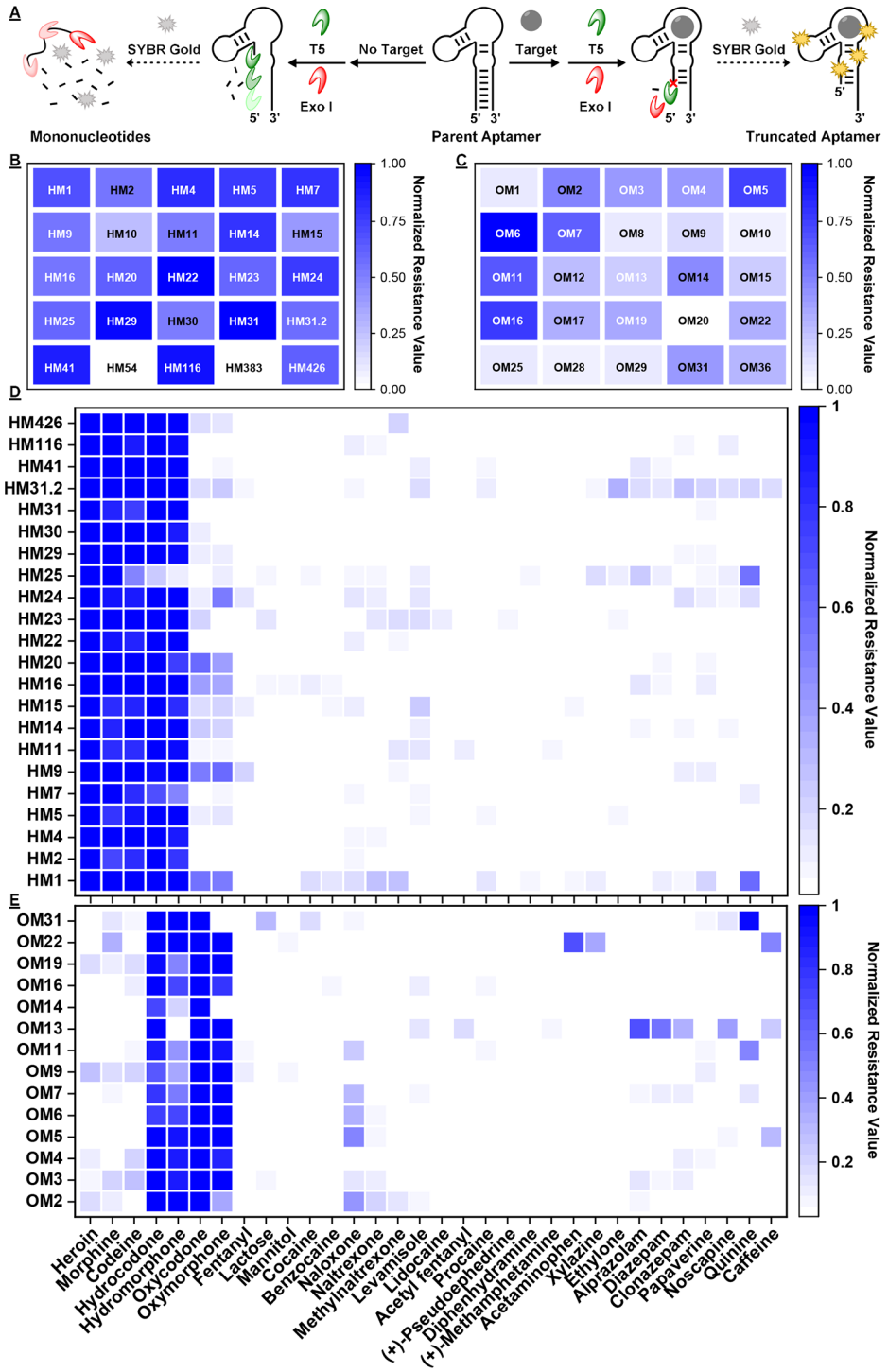

Figure 3. Use of exonuclease digestion fluorescence assays to determine the binding profile of opioid aptamers. (A) Scheme for the T5 Exo/Exo I fluorescence assay. (B, C) Resistance values for HM and OM aptamers in the presence of 100 μM heroin and 100 μM oxycodone, respectively. (D, E) Specificity of HM and OM aptamers for various opioids and interferents as determined using the T5 Exo/Exo I fluorescence assay. Heroin, morphine, codeine, hydrocodone, hydromorphone, oxycodone, and oxymorphone were tested at 100 μM. Interferents were tested at a concentration of 250 μM, except for alprazolam, diazepam, clonazepam, papaverine, and noscapine, which were tested at 100 μM in solution containing 1% MeOH. Data are presented as heat maps, with each square representing one aptamer and color intensity corresponding to resistance value. Increasing color intensity indicates higher resistance values and hence tighter aptamer-ligand binding. We performed two independent trials, and the data represented here represent the average from all trials.

<15% cross-reactivity. Among these, OM4, OM9, OM14, OM16, and OM19 had zero cross-reactivity to naloxone, which is impressive given the high degree of structural similarity between oxycodone/oxymorphone and naloxone. Other OM aptamers had poorer specificity, particularly against naloxone (Figure 3E).

Based on these data, we identified three different types of cross-reactive aptamers with a particular pattern of preference

https://doi.org/10.1021/jacsau.3c00801
JACS Au 2024, 4, 1059−1072

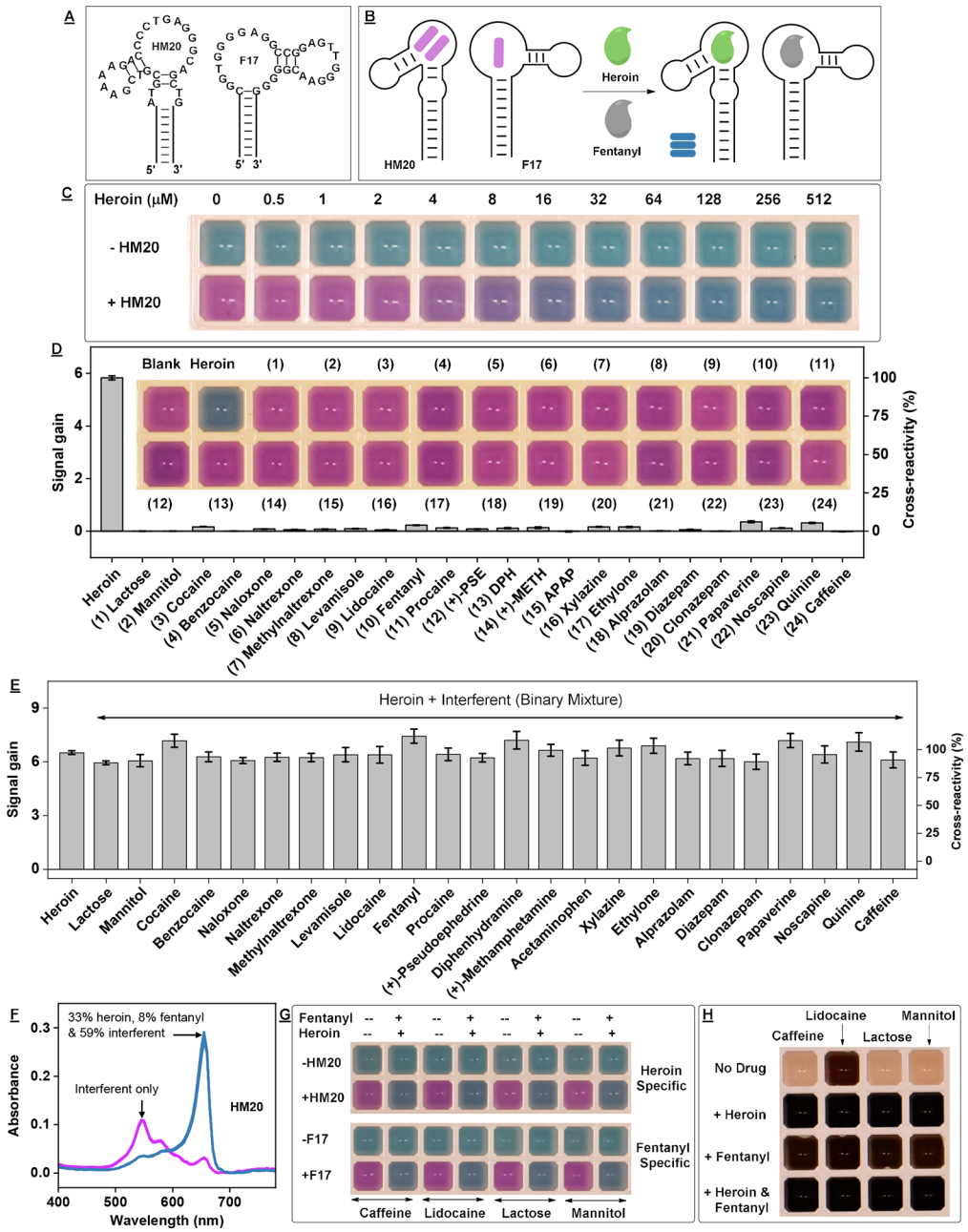

Figure 4. Detection of heroin and fentanyl using aptamer-based dye-displacement assays. (A) Secondary structures of HM20 and F17 based on NUPACK predictions. (B) Scheme of the dye-displacement assay using HM20, F17, and MTC (purple bars indicate monomeric/dimeric forms of the dye; blue bars indicate *J*-aggregates). (C) Photographs taken 5 min after addition of various concentrations of heroin to solutions of MTC alone (−HM20) or HM20-MTC complexes (+HM20). (D) Signal gain and cross-reactivity of the displacement assay to various interferents relative to the response to heroin. Photographs of samples were taken 5 min after adding mixtures of 25 μM heroin and 50 μM interferent to HM20-MTC complexes. (E) Detection of heroin in binary mixtures of 25 μM heroin (~33%) with 50 μM interferent (~67%). (F) Absorbance spectra of HM20-MTC complexes in the presence of a 33:8:59 mixture of heroin, fentanyl, and an interferent (caffeine, lidocaine, lactose, or mannitol) as well as each interferent alone. These spectra overlap for all four drug mixtures and all four interferent samples. (G) Photographs of the dye-displacement assays analyzed in panel F (top) as well as equivalent assays performed with the fentanyl-specific aptamer F17 (bottom). (H) Photographs of Marquis test results for interferent alone, binary mixtures containing heroin and interferent (33:67) or fentanyl and interferent (8:92), or ternary mixtures containing heroin, fentanyl, and interferent (33:8:59). Error bars represent the standard deviations of three independent experiments.

for the opioid targets. The first, which includes most HM aptamers (of which HM20 was the best performing), binds to opioids containing hydrogen at C14, such as morphine, codeine, hydrocodone, and hydromorphone with >90% cross-reactivity relative to heroin. However, they do not recognize opioids with a hydroxyl group at C14, such as oxycodone and oxymorphone, or the opioid antagonists naloxone, naltrexone, and methylnaltrexone. This information, along with the fact that the aptamers tolerate substitutions at C3 and C6 and have no preference for the double bond between C7 and C8, indicates that most HM aptamers interact with the A, B, and D rings of opioids, where substituents at C3 and C6 most likely face away from the aptamer and toward the solution. The second type, of which OM9 has the best affinity

https://doi.org/10.1021/jacsau.3c00801
JACS Au 2024, 4, 1059−1072

and specificity, recognizes opioids with a C14 hydroxyl group, such as oxycodone and oxymorphone, with similar levels of affinity and exhibits less cross-reactivity (≤50%) to hydrocodone and hydromorphone, which lack the hydroxyl group at C14 but retain the C6 ketone group. However, these aptamers did not bind morphine, heroin, or codeine, which lacked both of these groups. The moderate cross-reactivity of OM9 to naloxone demonstrates that the hydroxyl group at C14 is important for binding, whereas bulky substituents at the amino group decrease the affinity. The intolerance of the aptamer for such substituents is further evidenced by the complete lack of affinity for naltrexone and methylnaltrexone, which feature a methyl cyclopropyl substituent. The third aptamer type, of which OM4 was the best performer, bound oxymorphone, hydrocodone, and hydromorphone with >90% cross-reactivity relative to oxycodone, but had no affinity to morphine, heroin, or codeine, which all lack the C6 ketone. This indicates that the keto moiety on the C ring is an essential interaction point for this aptamer, and its tolerance to variation at C6 and C14 suggests that it primarily interacts with the C and D ring systems of opioid molecules.

Aptamer-Based Dye Displacement Assay for Colorimetric Detection of Morphine-Related Opioids

We used HM20, the aptamer with the highest affinity and specificity from our selections (Figure 4A), to develop colorimetric aptamer-based dye-displacement assays[21] for on-site detection of opioids in seized substances and counterfeit pills. Based on our previous work, we employed the DNA-binding cyanine dye 3,3′-di(3-sulfopropyl)-4,5,4′,5′-dibenzo-9-methyl-thiacarbocyanine (MTC),[39,40] which binds aptamers as monomers and dimers in the absence of target. When the target is added to the aptamer-dye complex, the dye is liberated into solution and forms *J*-aggregates, resulting in a purple-to-blue color change (Figure 4B). To detect heroin, we first optimized the concentration of HM20 required to deplete MTC aggregates and form aptamer-dye complexes by mixing 2.5 μM MTC with various concentrations of the aptamer (0−10 μM) in aqueous buffer. We observed an increase in monomer and dimer absorbance at 585 and 550 nm, respectively, and a decrease in *J*-aggregates that absorb maximally at 650 nm as a function of aptamer concentration, with nearly 90% bound to the aptamer at ∼6 μM aptamer (Figure S21). Notably, unlike other aptamers we have tested with MTC previously,[32] HM20 prefers to bind MTC dimers as opposed to monomers. Since the dimer has an absorbance peak that is farther from the *J*-aggregate absorbance peak, this potentially increases the assay color contrast to allow for more confident identification of a color change with the naked eye.

We then challenged the aptamer-dye complexes with varying concentrations of heroin (0−512 μM) and observed a target-concentration-dependent increase in *J*-aggregate absorbance and decreases in dimer and monomer absorbance (Figure S22A). To quantify the signal change, we calculated the ratio between the AUC of the absorbance spectra between 590−680 nm (for *J*-aggregates) and 500−590 nm (for monomers/dimers). Using this ratio, we calculated signal gains and plotted these values as a function of target concentration to construct a calibration curve (Figure S22B). Based on these data, the assay had an instrumental limit of detection of 0.5 μM with a linear range from 0−16 μM (Figure S22C). A control experiment performed by mixing the dye with varying concentrations of heroin demonstrated that the target itself does not perturb the dye aggregation state or absorbance spectra (Figure S22D). Notably, the presence of heroin can be clearly identified at concentrations as low as 8 μM with the naked eye via a purple-to-blue-green color change (Figure 4C), which is sufficiently sensitive for detecting opioids in seized drug samples. We then determined the specificity of the assay against a variety of ligands commonly found in illicit drug samples. Since the purity of heroin is often 30−50%,[41,42] we assessed the specificity of our assay by challenging aptamer-dye complexes with 25 μM heroin or 50 μM interferent. The assay did not have any meaningful cross-reactivity to any of these interferents, and only the heroin sample induced a purple-to-blue-green color change that was visible to the naked eye (Figure 4D). We then challenged the assay with binary mixtures of 25 μM heroin (∼33%) and 50 μM interferent (∼67%) and did not observe that any of these interferents altered the signal produced by heroin, demonstrating the excellent specificity of the assay (Figure 4E).

Heroin, among other drugs, is increasingly being laced with fentanyl.[41] To determine if our assay could specifically detect heroin in drug mixtures, we combined heroin (33%; 25 μM) with fentanyl (8%; 6 μM) and one of four common cutting agents, caffeine, lidocaine, lactose, or mannitol (59%; 45 μM). We challenged the HM20-based dye-displacement assay with these mixtures and found that the assay could specifically and accurately detect heroin, even in the presence of cutting agents and fentanyl (Figure 4F). More impressively, the color produced in fentanyl-containing samples (Figure 4G, heroin specific) was almost identical to fentanyl-free samples (Figure S23). To determine if our assay could detect both heroin and fentanyl, we utilized our recently isolated aptamer F17, which binds fentanyl with nanomolar affinity, to detect this drug in these drug mixtures.[22,23] The F17-based MTC-displacement assay could detect fentanyl via a purple-to-blue-green color change despite its low quantity in the drug mixture regardless of the absence (Figure S24) or presence of heroin (Figures S25 and 4G, fentanyl specific), without any response to other interferents. These results are consistent with ITC data indicating that HM20 does not bind to fentanyl (Figure S26A) and F17 does not bind heroin (Figure S26B). Our aptamer-based dye-displacement assays thus enable visual detection of heroin and fentanyl in a specific and sensitive manner, even in complex mixtures containing both drugs and other interferents.

Our aptamer-based dye-displacement assays are much more specific and selective for drug testing relative to the widely used Marquis test for opioids.[4,6,7] To demonstrate this, we detected heroin and fentanyl alone or in a binary mixture together with one other interferent (lactose, lidocaine, caffeine, or mannitol) as well as each interferent alone. When challenged with the Marquis reagent, the interferents yielded a nearly colorless solution, except for lidocaine, which produced a brown color, (Figure 4H). Binary mixtures containing 33% heroin and 67% interferent yielded a dark purple color (Figure 4H), which matches the characteristic color heroin produces in the Marquis test (Figure S27). Binary mixtures containing 8% fentanyl and 92% interferent turned dark brown (Figure 4H), which is the signature color of fentanyl for this test (Figure S27). However, given that fentanyl and lidocaine yield similar colors, it is not possible to differentiate between drug-positive and drug-negative results with this interferent. In ternary mixtures containing 8% fentanyl, 33% heroin, and 59% interferent, the dark purple

https://doi.org/10.1021/jacsau.3c00801
JACS Au 2024, 4, 1059−1072

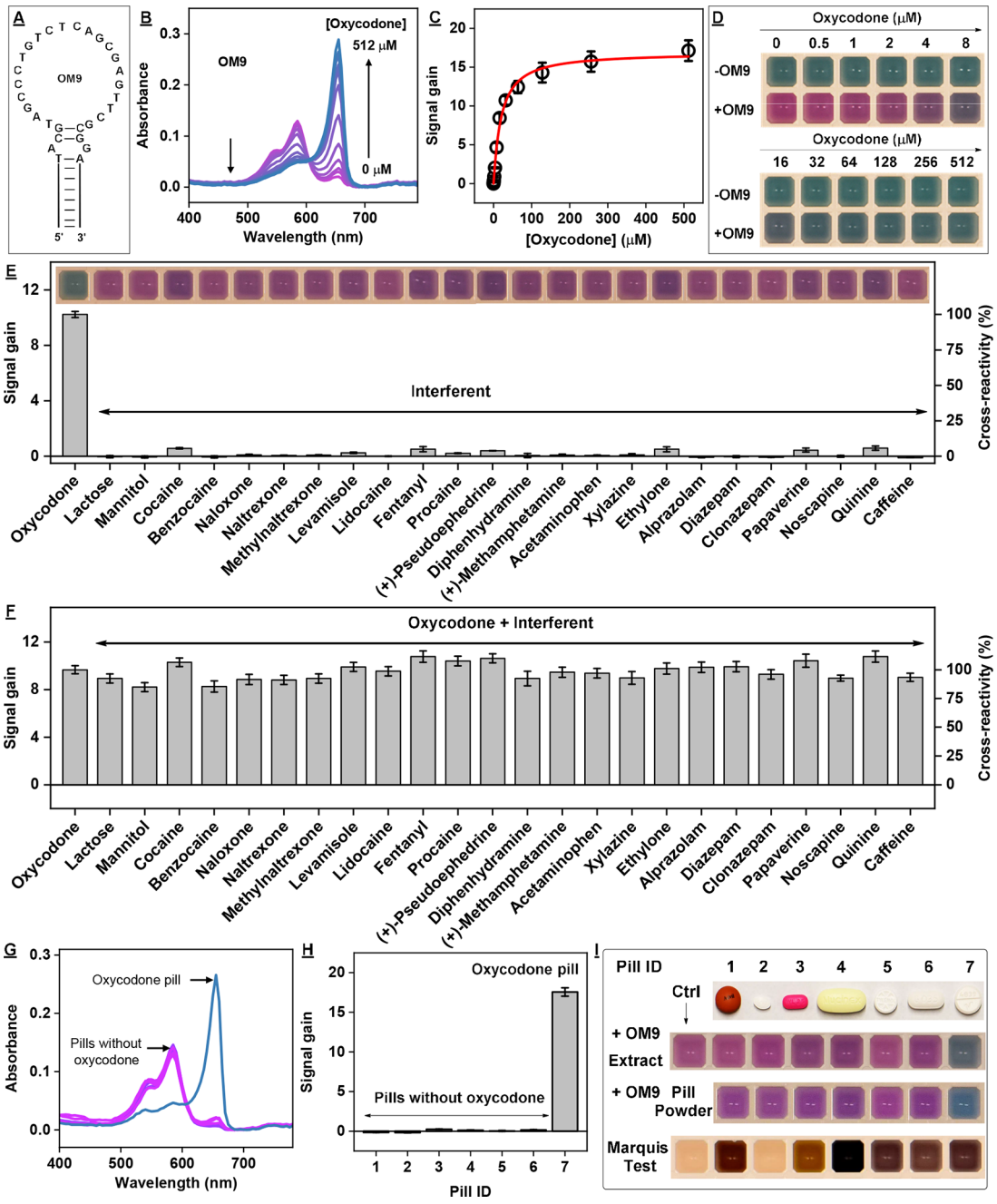

Figure 5. Utilizing the dye-displacement assay and OM9 to detect oxycodone. (A) Secondary structure of OM9 based on NUPACK prediction. (B) Absorbance spectra of OM9-MTC complexes in the presence of various concentrations of oxycodone, with the purple-to-blue-green color gradient representing increasing concentrations. (C) Calibration curve for oxycodone detection. (D) Photographs taken 5 min after addition of various concentrations of oxycodone to solutions of MTC alone (−OM9) or OM9-MTC complexes (+OM9). (E) Assay specificity against 25 μM oxycodone or 50 μM interferent, with cross-reactivity shown relative to oxycodone. (F) Assay response to binary mixtures of 25 μM oxycodone and 50 μM interferent. (G) Absorbance spectra of OM9-MTC complexes challenged with oxycodone tablet extract as well as extracts of six other prescription or over-the-counter drugs. (H) Quantified assay response to these extracts, and (I) photographs of the aptamer-based MTC-displacement assay results for both extensively processed pill extracts (top) and minimally processed pill powders (middle), as well as Marquis test results for each pill powder. In panels H and I, numbered tablets are (1) Advil, (2) Claritin, (3) Benadryl, (4) Mucinex, (5) Tylenol, (6) generic hydrocodone/acetaminophen, and (7) generic oxycodone/acetaminophen. Error bars represent the standard deviation of three independent experiments.

color produced by heroin completely masked the color produced by fentanyl, resulting in a true positive for heroin but a false negative for fentanyl. These results highlight the insufficiencies of this standard chemical test for forensic drug testing and demonstrate the added value that aptamer-based tests can bring to the field.

We next developed an MTC displacement assay using OM9 (Figure 5A) for the detection of oxycodone. Aptamer optimization experiments indicated that 85% of the dye was bound to the aptamer at 4 μM OM9 (Figure S28). We then challenged the aptamer-dye complexes with various concentrations of oxycodone (0−512 μM) (Figure 5B,C) and were

https://doi.org/10.1021/jacsau.3c00801
JACS Au 2024, 4, 1059−1072

able to observe a color change with the naked eye at 8 μM oxycodone (Figure 5D), with an instrumental detection limit of 0.5 μM and a linear range from 0 to 16 μM (Figure S29). Control experiments confirmed that oxycodone itself does not perturb the aggregation state or absorbance spectrum of the dye in the absence of aptamer OM9 (Figure S30). We also determined the specificity of the assay by challenging MTC-OM9 complexes with 25 μM oxycodone or 50 μM of a wide range of interferents. OM9 demonstrated excellent specificity, with little to no response to any of the interferent molecules and only oxycodone produced a visible purple-to-blue-green color change (Figure 5E). Finally, we challenged the assay with binary mixtures of 25 μM oxycodone and 50 μM interferent and observed identical color changes and signal response from oxycodone, whether or not interferents were present (Figure 5F).

Diversion and counterfeiting of prescription opioid pills containing oxycodone and hydrocodone have been major contributors to the opioid epidemic. We assessed whether the OM9 dye-displacement assay could accurately differentiate legitimate opioid-containing prescription medicines from other pharmaceutical tablets. Specifically, we tested the response of the assays to a 5 mg hydrocodone tablet containing 325 mg acetaminophen and a 5 mg oxycodone tablet with 325 mg acetaminophen, as well as other common over-the-counter drugs including Advil (200 mg ibuprofen), Claritin (10 mg loratadine), Benadryl (25 mg diphenhydramine), Mucinex (60 mg dextromethorphan and 1200 mg guaifenesin), and Tylenol (325 mg acetaminophen). First, as a proof of concept, we performed a standardized laboratory-based extraction protocol to assess whether our assay could positively detect oxycodone from tablet extract solutions. The assay yielded a positive response to the oxycodone tablets, with a clear purple-to-blue-green color change, and little to no response to the other tablets (Figure 5G–I). This is impressive as dextromethorphan, the active ingredient in Mucinex, has a high degree of structural similarity to oxycodone. Another advantage of the dye-displacement assay is that, due to its high sensitivity, we could heavily dilute colored interferences (e.g., in Advil, Benadryl, and Mucinex tablets) while still being able to detect the target via the naked eye (Figure 5I).

Having established that our assay could detect extracted oxycodone from a tablet, we next established a facile dye displacement protocol that can be used in field settings by laypersons. The tablets were first cut in half and then mixed with 10% methanol in water, shaking vigorously for 1 min, effectively breaking the pill down into a slurry. Then, the solution was mixed with an aptamer dye solution, which caused an instantaneous change in color from purple to blue (Figure 5I, pill powder). In contrast, we observed no color change for the pharmaceutical tablets that did not contain oxycodone. With Benadryl, we did note a slight red hue in the solution, which can be attributed to the coloring agents from the pink tablet itself, but the result was nevertheless unambiguously negative. We also performed the Marquis test on the same panel of tablets (Figure 5I, Marquis test). Advil and Bendaryl, which respectively contain ibuprofen and diphenhydramine, yielded orange-brown colors that could be easily mistaken for the readout produced by fentanyl, highlighting the test's lack of specificity. In addition, Mucinex produced a black color, mainly due to the presence of dextromethorphan, which could be confused with a positive readout for heroin. Finally, the Tylenol tablet and oxycodone tablet both yielded the same purple-brown color, indicating that the two tablets cannot be distinguished from each other or other licit tablets. Clearly, our aptamer-based dye displacement assays offer a superior on-site screening test for differentiating actual opioid-containing tablets from other over-the-counter or prescription medicines.

CONCLUSIONS

We performed in vitro selection to isolate DNA aptamers that bind to morphine-related opioids. Our aptamers bind to these targets with submicromolar to micromolar affinity and have excellent specificity. Based on our previous experience obtaining nanomolar-affinity aptamers for small-molecule targets, we expected that we would obtain opioid-binding aptamers with $K_D \leq 100$ nM due to the abundance of functional groups contained by morphine-like opioids including aromatic rings, amines, hydroxyls, and carbonyls. However, the aptamers we isolated here only had an average K_D of 1 μM. The Smolke group previously isolated RNA aptamers for codeine with K_D of 2.5–4.0 μM,[43] which suggests that aptamers may generally face difficulty binding to bulky molecules like morphinan opioids. This may not be strictly true, however, since aptamers have been reported recently that bind oxycodone and hydrocodone with nanomolar affinity.[44] Unfortunately, the sequences of these aptamers—as well as their specificity against a diverse range of interferents—were not reported. Notably, both our selections and those performed by the Smolke group entailed counter-SELEX against nontargets that were very structurally similar to the selection targets. In this work, we used naloxone, naltrexone, and methylnaltrexone, whereas the Smolke group performed counterselection against morphine. We hypothesize that the use of counter-targets with a high degree of structural similarity to the target can eliminate high-affinity aptamers from the library that happen to recognize functional groups shared by the target and counter-targets. This hypothesis is also supported by our experience with the isolation of highly specific aptamers for the stimulant 4-methylmethcathinone, in which we performed counter-SELEX against numerous structurally similar molecules such as 4-methoxymethcathinone; the resulting aptamers only had micromolar affinity.[31]

Since we focus on the detection of opioids in seized substances, the specificity of the aptamer assay becomes much more significant relative to its LOD given that the drug will almost always be present at fairly considerable concentrations in a true-positive scenario involving actual contraband or prescription medications. Here, we were able to successfully utilize the newly isolated HM20 and OM9 aptamers and the organic dye MTC to develop dye displacement assays for detecting opioids. In general, these assays are not only sensitive and specific but also rapid—requiring only seconds for a color change—and easy to perform onsite. We demonstrated that these assays could detect oxycodone, heroin, and fentanyl in complex mixtures with a purple-to-blue-green color change without meaningful interference or matrix effects. For instance, using HM20 and the fentanyl-binding aptamer F17, we could accurately detect the presence of 33% heroin and 8% fentanyl, respectively, in the presence of ~60% interferent without any crosstalk. We also showcased the ability of our assay to identify oxycodone in prescription tablets without any false positives to commonly used over-the-counter medications, including ibuprofen, loratadine, diphenhydramine, acetaminophen, and dextromethorphan/guaifenesin. These results highlight both

https://doi.org/10.1021/jacsau.3c00801
JACS Au 2024, 4, 1059–1072

the excellent specificity of our aptamers and the robustness of the dye-displacement assay platform. These assays are superior for on-site drug testing relative to conventional chemical drug tests such as the Marquis test for several reasons. First, and most importantly, chemical tests can yield similar color responses to nontarget compounds, resulting in false positives—including from legal, commonly used medications like Tylenol. Second, when drugs are heavily cut with other illicit drugs, cutting agents, or adulterants, the color produced by the target in question can be masked or mixed with colors produced by other substances in the mixture, resulting in false negatives. Our assay is therefore significant because it has solved a long-standing problem that no other in-field analytical approaches could address. We also demonstrated that our test can be performed by simply mixing the aptamer-dye solution with a crushed and dissolved drug sample and observing an immediate color change by the naked eye. We believe that this assay is therefore feasible for first responders and law enforcement personnel to augment drug interdiction efforts and prevent harm associated with the consumption of opioid-adulterated substances.

■ ASSOCIATED CONTENT

Data Availability Statement

High-throughput DNA sequencing data can be found online at the NIH Sequencing Read Archive by using the name of this paper.

Supporting Information

The Supporting Information is available free of charge at https://pubs.acs.org/doi/10.1021/jacsau.3c00801.

Sequences of DNA used in this work, selection conditions, summary of aptamer sequences and aptamer dissociation constants and ITC conditions, chemical structure of interferents employed in counter-SELEX, binding affinity of SELEX pools, proportion of unique sequences in pools, ITC data for HM and OM aptamers, optimizing aptamer-dye ration for dye-displacement assays, detection of heroin, fentanyl, and oxycodone using MTC-based displacement assays, and the effect of oxycodone or heroin on the absorbance spectrum of MTC alone (PDF)

■ AUTHOR INFORMATION

Corresponding Author

Yi Xiao − *Department of Chemistry, North Carolina State University, Raleigh, North Carolina 27695, United States;* orcid.org/0000-0001-7278-9811; Email: yxiao34@ncsu.edu

Authors

Juan Canoura − *Department of Chemistry, North Carolina State University, Raleigh, North Carolina 27695, United States*

Obtin Alkhamis − *Department of Chemistry, North Carolina State University, Raleigh, North Carolina 27695, United States*

Matthew Venzke − *Department of Chemistry, North Carolina State University, Raleigh, North Carolina 27695, United States*

Phuong T. Ly − *Department of Chemistry, North Carolina State University, Raleigh, North Carolina 27695, United States;* orcid.org/0000-0003-2788-4443

Complete contact information is available at: https://pubs.acs.org/10.1021/jacsau.3c00801

Notes

The authors declare no competing financial interest.

■ ACKNOWLEDGMENTS

This work was supported by the National Institute of Justice, Grant Office of Justice Programs, U.S. Department of Justice Award 2019-DU-BX-0024 and 2022-GG-04440-RESS.

■ REFERENCES

(1) Kozitsina, A. N.; Svalova, T. S.; Malysheva, N. N.; Okhokhonin, A. V.; Vidrevich, M. B.; Brainina, K. Z. Sensors Based on Bio and Biomimetic Receptors in Medical Diagnostic, Environment, and Food Analysis. *Biosensors* **2018**, *8*, 35.

(2) de Oliveira, L. P.; Rocha, D. P.; de Araujo, W. R.; Muñoz, R. A. A.; Paixão, T. R. L. C.; Salles, M. O. Forensics in Hand: New Trends in Forensic Devices (2013−2017). *Anal. Methods* **2018**, *10*, 5135−5163.

(3) Philp, M.; Fu, S. A Review of Chemical 'Spot' Tests: A Presumptive Illicit Drug Identification Technique. *Drug Test Anal.* **2018**, *10*, 95−108.

(4) O'Neal, C. L.; Crouch, D. J.; Fatah, A. A. Validation of Twelve Chemical Spot Tests for the Detection of Drugs of Abuse. *Forensic Sci. Int.* **2000**, *109*, 189−201.

(5) Auterhoff, H.; Braun, D. Die Farbreaktion Des Morphins Nach E MARQUIS. *Arch. Pharm.* **1973**, *306*, 866−872.

(6) Reno, J.; Marcus, D.; Leary, M. L.; Samuels, J. E. *Color Test Reagents/Kits for Preliminary Identification of Drugs of Abuse. NIJ. Standard-0604.01* 1981.

(7) Marinetti, L. J.; Ehlers, B. J. A Series of Forensic Toxicology and Drug Seizure Cases Involving Illicit Fentanyl Alone and in Combination with Heroin, Cocaine or Heroin and Cocaine. *J. Anal. Toxicol.* **2014**, *38*, 592−598.

(8) Lockwood, T.-L. E.; Vervoordt, A.; Lieberman, M. High Concentrations of Illicit Stimulants and Cutting Agents Cause False Positives on Fentanyl Test Strips. *Harm Reduct. J.* **2021**, *18*, 30.

(9) West, M. J.; Went, M. J. Detection of Drugs of Abuse by Raman Spectroscopy. *Drug Test. Anal.* **2011**, *3*, 532−538.

(10) Hargreaves, M. D.; Burnett, A. D.; Munshi, T.; Cunningham, J. E.; Linfield, E. H.; Davies, A. G.; Edwards, H. G. M. Comparison of near Infrared Laser Excitation Wavelengths and Its Influence on the Interrogation of Seized Drugs-of-Abuse by Raman Spectroscopy. *J. Raman Spectrosc.* **2009**, *40*, 1974−1983.

(11) Liu, C.-M.; He, H.-Y.; Xu, L.; Hua, Z.-D. New Qualitative Analysis Strategy for Illicit Drugs Using Raman Spectroscopy and Characteristic Peaks Method. *Drug Test. Anal.* **2021**, *13*, 720−728.

(12) Haddad, A.; Comanescu, M. A.; Green, O.; Kubic, T. A.; Lombardi, J. R. Detection and Quantitation of Trace Fentanyl in Heroin by Surface-Enhanced Raman Spectroscopy. *Anal. Chem.* **2018**, *90*, 12678−12685.

(13) Černý, J.; Hobza, P. Non-Covalent Interactions in Biomacromolecules. *Phys. Chem. Chem. Phys.* **2007**, *9*, 5291−5303.

(14) National Research Council. *Monoclonal Antibody Production*; The National Academies Press: Washington, DC. 1999.

(15) Dunn, M. R.; Jimenez, R. M.; Chaput, J. C. Analysis of Aptamer Discovery and Technology. *Nat. Rev. Chem.* **2017**, *1*, No. 0076.

(16) Tuerk, C.; Gold, L. Systematic Evolution of Ligands by Exponential Enrichment: RNA Ligands to Bacteriophage T4 DNA Polymerase. *Science* **1990**, *249*, 505−510.

(17) Ellington, A. D.; Szostak, J. W. *In Vitro* Selection of RNA Molecules That Bind Specific Ligands. *Nature* **1990**, *346*, 818−822.

(18) Jenison, R. D.; Gill, S. C.; Pardi, A.; Polisky, B. High-Resolution Molecular Discrimination by RNA. *Science* **1994**, *263*, 1425−1429.
(19) Yang, W.; Yu, H.; Alkhamis, O.; Liu, Y.; Canoura, J.; Fu, F.; Xiao, Y. *In Vitro* Isolation of Class-Specific Oligonucleotide-Based Small-Molecule Receptors. *Nucleic Acids Res.* **2019**, *47*, No. e71.
(20) Xiao, Y.; Lubin, A. A.; Heeger, A. J.; Plaxco, K. W. Label-Free Electronic Detection of Thrombin in Blood Serum by Using an Aptamer-Based Sensor. *Angew. Chem., Int. Ed.* **2005**, *44*, 5456−5459.
(21) Stojanovic, M. N.; Landry, D. W. Aptamer-Based Colorimetric Probe for Cocaine. *J. Am. Chem. Soc.* **2002**, *124*, 9678−9679.
(22) Canoura, J.; Alkhamis, O.; Liu, Y.; Willis, C.; Xiao, Y. High-Throughput Quantitative Binding Analysis of DNA Aptamers Using Exonucleases. *Nucleic Acids Res.* **2023**, *51*, No. e19.
(23) Canoura, J.; Liu, Y.; Perry, J.; Willis, C.; Xiao, Y. Suite of Aptamer-Based Sensors for the Detection of Fentanyl and Its Analogues. *ACS Sens.* **2023**, *5*, 1901−1911.
(24) White, R.; Rusconi, C.; Scardino, E.; Wolberg, A.; Lawson, J.; Hoffman, M.; Sullenger, B. Generation of Species Cross-Reactive Aptamers Using "Toggle" SELEX. *Mol. Ther.* **2001**, *4*, 567−573.
(25) Wang, Z.; Yu, H.; Canoura, J.; Liu, Y.; Alkhamis, O.; Fu, F.; Xiao, Y. Introducing Structure-Switching Functionality into Small-Molecule-Binding Aptamers via Nuclease-Directed Truncation. *Nucleic Acids Res.* **2018**, *46*, No. e81.
(26) Alkhamis, O.; Canoura, J.; Ly, P. T.; Xiao, Y. Using Exonucleases for Aptamer Characterization, Engineering, and Sensing. *Acc. Chem. Res.* **2023**, *56*, 1731−1743.
(27) Yang, K.-A.; Pei, R.; Stojanovic, M. N. *In Vitro* Selection and Amplification Protocols for Isolation of Aptameric Sensors for Small Molecules. *Methods* **2016**, *106*, 58−65.
(28) Yu, H.; Yang, W.; Alkhamis, O.; Canoura, J.; Yang, K.-A.; Xiao, Y. In Vitro Isolation of Small-Molecule-Binding Aptamers with Intrinsic Dye-Displacement Functionality. *Nucleic Acids Res.* **2018**, *46*, No. e43.
(29) Martin, M. Cutadapt Removes Adapter Sequences from High-Throughput Sequencing Reads. *EMBnet J.* **2011**, *17*, 10−12.
(30) Alam, K. K.; Chang, J. L.; Burke, D. H. FASTAptamer: A Bioinformatic Toolkit for High-Throughput Sequence Analysis of Combinatorial Selections. *Mol. Ther.–Nucleic Acids* **2015**, *4*, No. e230.
(31) Alkhamis, O.; Yang, W.; Farhana, R.; Yu, H.; Xiao, Y. Label-Free Profiling of DNA Aptamer-Small Molecule Binding Using T5 Exonuclease. *Nucleic Acids Res.* **2020**, *48*, No. e120.
(32) Alkhamis, O.; Canoura, J.; Bukhryakov, K. V.; Tarifa, A.; DeCaprio, A. P.; Xiao, Y. DNA Aptamer−Cyanine Complexes as Generic Colorimetric Small-Molecule Sensors. *Angew. Chem., Int. Ed.* **2022**, *61*, No. e20211305.
(33) Masotti, L.; Avitabile, M.; Barcellona, M. L.; Von Berger, J.; Manca, N.; Turano, A. Interaction of Papaverine with Covalently Closed DNA. *Microbiologica* **1985**, *8*, 263−268.
(34) Maurya, N.; Alzahrani, K. A.; Patel, R. Probing the Intercalation of Noscapine from Sodium Dodecyl Sulfate Micelles to Calf Thymus Deoxyribose Nucleic Acid: A Mechanistic Approach. *ACS Omega* **2019**, *4*, 15829−15841.
(35) Quang, N. N.; Bouvier, C.; Henriques, A.; Lelandais, B.; Ducongé, F. Time-Lapse Imaging of Molecular Evolution by High-Throughput Sequencing. *Nucleic Acids Res.* **2018**, *46*, 7480−7494.
(36) Cowan, J. A.; Ohyama, T.; Wang, D.; Natarajan, K. Recognition of a Cognate RNA Aptamer by Neomycin B: Quantitative Evaluation of Hydrogen Bonding and Electrostatic Interactions. *Nucleic Acids Res.* **2000**, *28*, 2935−2942.
(37) U.S. Department of Justice Drug Enforcement Agency. *2016 Heroin Domestic Monitor Program DEA Intelligence Report. DEA-DCW-DIR-026−18*, 2018.
(38) U.S. Department of Justice Drug Enforcement Agency. *Fentanyl Signature Profiling Program Report. DEA PRB 10−25−19−40*, 2019.
(39) Sun, H.; Xiang, J.; Gai, W.; Shang, Q.; Li, Q.; Guan, A.; Yang, Q.; Liu, Y.; Tang, Y.; Xu, G. Visual Detection of Potassium by a Cyanine Dye Supramolecular Aggregate Responsive to G-Quadruplex Motif Transition. *Analyst* **2012**, *137*, 5713−5715.
(40) Yang, C.; Yang, S.; Song, L.; Yao, Y.; Lin, X.; Cai, K.; Yang, Q.; Tang, Y. A Resettable Supramolecular Platform for Constructing Scalable Encoders. *Chem. Commun.* **2019**, *55*, 8005−8008.
(41) Diversion Control Division. *National Forensic Laboratory Information System: NFLIS-Drug 2022 annual report*; Department of Justice, U.S. Drug Enforcement Administration: U.S., 2023.
(42) Palamar, J. J.; Ciccarone, D.; Rutherford, C.; Keyes, K. M.; Carr, T. H.; Cottler, L. B. Trends in Seizures of Powders and Pills Containing Illicit Fentanyl in the United States, 2018 through 2021. *Drug Alcohol Depend.* **2022**, *234*, No. 109398.
(43) Win, M. N.; Klein, J. S.; Smolke, C. D. Codeine-Binding RNA Aptamers and Rapid Determination of Their Binding Constants Using a Direct Coupling Surface Plasmon Resonance Assay. *Nucleic Acids Res.* **2006**, *34*, 5670−5682.
(44) Kammer, M. N.; Kussrow, A.; Gandhi, I.; Drabek, R.; Batchelor, R. H.; Jackson, G. W.; Bornhop, D. J. Quantification of Opioids in Urine Using an Aptamer-Based Free-Solution Assay. *Anal. Chem.* **2019**, *91*, 10582−10588.

https://doi.org/10.1021/jacsau.3c00801
JACS Au 2024, 4, 1059−1072